A Knowledge-Based Optimization Method for Aerodynamic Design

Richard L. Campbell [1] and Michelle N. Lynde [2]
NASA Langley Research Center, Hampton, Virginia, 23681

A new aerodynamic design method, CODISC, has been developed that combines a legacy knowledge-based design method, CDISC, with a simple optimization module known as SOUP. The primary goal of this new design system is to improve the performance gains obtained using CDISC without adding significant computational time. An additional objective of this approach is to reduce the need for *a priori* knowledge of good initial input variable values, as well as for subsequent manual revisions of those values as the design progresses. Several test cases illustrate the development of the process to date and some of the options available at transonic and supersonic speeds for turbulent flow designs. The test cases generally start from good baseline configurations and, in all cases, were able to improve the performance. Several new guidelines for good initial values for the design variables, as well as new design rules within CDISC itself, were developed from these cases.

Nomenclature

Acronyms

AOWDG	=	Aerodynamic Optimization Workshop Discussion Group
CART3D	=	Cartesian 3-D, Euler flow solver
CDISC	=	Constrained Direct Iterative Surface Curvature, design module
CF	=	Crossflow boundary layer mode
CFD	=	Computational Fluid Dynamics
CODISC	=	Constrained Optimization Direct Iterative Surface Curvature, design system
D0	=	Supercritical airfoil test case
LASTRAC	=	Langley Stability and Transition Analysis Code, transition prediction software
MSES	=	2-D Euler with interacted boundary layer flow solver
CRM	=	Common Research Model
NJWB	=	NASA/JAXA Wing Body, supersonic configuration test case
NLF	=	Natural laminar flow
PADRI	=	Platform for Aircraft Drag Reduction Innovation
SOUP	=	Simple Optimization Utility Program, optimization module
TS	=	Tollmien-Schlichting boundary layer mode
USM3D	=	Unstructured Mesh 3D, Navier-Stokes flow solver

Symbols

c	=	Chord length
C_D	=	Configuration drag coefficient
c_d	=	Sectional drag coefficient
C_L	=	Configuration lift coefficient
c_l	=	Sectional lift coefficient
C_m	=	Configuration pitching-moment coefficient
c_m	=	Sectional pitching moment coefficient
C_P	=	Pressure coefficient
M_{1n}	=	Mach number component upstream and normal to the shock
V_l	=	midchord pressure gradient parameter in target pressure architecture
x/c	=	x-location nondimensionalized by local chord
X_{ca}	=	x/c location of end of crossflow attenuation region in target pressure architecture
X_{tr}	=	x/c location of boundary layer transition in target pressure architecture

[1] Senior Research Engineer, NASA Langley Research Center M/S 499 Hampton, VA 23681, AIAA Associate Fellow.
[2] Research Aerospace Engineer, NASA Langley Research Center M/S 499 Hampton, VA 23681, AIAA Member.

X_{shk} = x/c location of shock in target pressure architecture
η = Semispan location

I. Introduction

THE use of automated CFD-based aerodynamic design methods has become the norm in the aircraft design process. The selection of a method is typically based on the three Es of a good design approach: Efficiency, Effectiveness, and Ease of use. A design method must be efficient enough to provide results within the time constraints of the design process. This implies not only a rapid design code, but also the flexibility to use different flow solvers, depending on the flight regime and the phase of design (e.g., conceptual or preliminary). The design approach must also be effective, providing the required accuracy while improving the configuration toward the design objective. Here efficiency can be an enabler by allowing larger, more accurate grids to be used in a timely fashion. Finally, the design system must be easy to use or the user base will be limited to an expert or two, or zero if the method is just too frustrating. Ease of use includes not only setting up the design case, but also having a robust process that does not require a lot of debugging and restarting of cases.

While the majority of the new methods being developed are based on numerical optimization, the knowledge-based CDISC design method [1] is still fairly widely used in US industry and government research organizations. The primary advantage of CDISC relative to a numerical optimization method is that, because it uses prescribed rather than computed sensitivity derivatives, it typically produces designs in about the same time as the original converged baseline analysis. Even with the use of an adjoint solver to compute these derivatives, optimization often requires 1-2 orders of magnitude more time than CDISC to produce a design. Nongradient-based optimization approaches, such as genetic methods, often require another order of magnitude or more time beyond the gradient-based methods.

A potential drawback of the knowledge-based approach to design is that it requires an *a priori* knowledge, not just of the flow physics that will lead to an improved design, but also of how to adjust the target pressures used in design to obtain the desired improvement while also meeting various constraints. In cases involving transonic transports, this knowledge base has been developed over the last few decades. As an illustration of this, CDISC was used to repeat the design cases for the Aerodynamic Optimization Workshop Discussion Group (AOWDG) W1 wing configuration reported by Vassberg [2]. The CDISC design philosophy was to make the spanload elliptical to minimize induced drag and to reduce shock strengths to decrease wave drag, while meeting the flow and geometry constraints. The final aggregate drag reductions for the dual-point design case from CDISC and the three optimization methods used in [2] are shown in figure 1. As can be seen, CDISC produced comparable drag reductions to the other optimization methods. This drag reduction was accomplished in much less time, as much as a factor of 500 relative to one of the other methods.

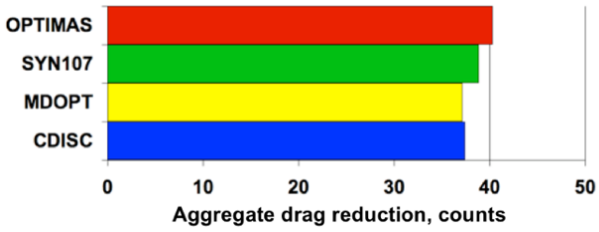

Figure 1. Design results for mulitpoint AWODG W1 case.

More recently, CDISC, along with other design and active flow control methods, was used in the PADRI 2018 Workshop [3] to try to reduce the drag of a generic strut-braced wing configuration at cruise. The design region was limited to a small area near the wing-strut junction and there were a number of other geometry and flow constraints. In the channel formed between the wing and strut near the junction, strong shocks and significant flow separations were present. For this problem, CDISC and a numerical optimization method [4] that used geometry reshaping produced the highest values of drag reductions obtained in the workshop, with each method achieving just over 13 counts of improvement.

The CDISC method uses flow constraints to generate target pressures based on design rules that have been developed from applications for a variety of configurations. Typically, the initial values of the input parameters are chosen based on previous experience, then are manually adjusted after several design cycles based on how the geometry and flow characteristics are developing. While this manual adjustment procedure has provided good results for a number of designs in the past, it is proposed that a more effective and efficient approach would be the use of optimization to determine the best CDISC input parameters.

This type of simple optimization approach with CDISC was first demonstrated by Campbell [5] for a transonic airfoil design. A more rigorous method that combines CDISC and optimization, known as KNOPTER, was developed by researchers formerly at Lockheed Martin and was successfully applied to several of their configurations [6,7]. For our new implementation of this approach, an auxiliary code, SOUP (Simple Optimization Utility Program), has been

created that adjusts the input parameters for selected CDISC flow constraints to try to reduce the drag of the configuration.

This hybrid approach, referred to as CODISC, is consistent with the overall emphasis on efficiency in CDISC and attempts to address the three Es. The primary objective is to improve the effectiveness of CDISC in terms of drag reduction. Even though CDISC often provides results that are comparable to those from numerical optimization, the target pressure architectures created by the flow constraints are not necessarily optimal. It is hoped that automatically adjusting one or more of the input parameters will provide some additional drag reduction and perhaps lead to new design rules that could reduce the need for these adjustments for future designs. The second objective is to retain as much of the original CDISC efficiency as possible, hopefully achieving optimized designs in less than 5x the time needed for the baseline analysis, or approximately double the time for a standard CDISC design. The final goal is to reduce the knowledge base required of the user in setting up the input for a design. While some input parameters have recommended values, these are increasingly less likely to be optimum for configurations that do not resemble the standard tube-and-wing transport aircraft used to develop the suggested values. With the new approach, it should be less important that the configuration coming out of conceptual design have refined wing twist and airfoil shapes.

II. Methods

A flow chart of the CODISC design system is shown in figure 2. The modular coupling of the original CDISC system has been retained to allow the use of multiple flow solvers and gridding approaches. For the examples included in this paper, three flow solvers were used: MSES [8], CART3D [9], and USM3D [10]. These flow solvers will be briefly described in the Results subsection where they are used. The new SOUP optimization and CDISC design modules and their interactions are described below. The transition information file loop is not needed for the cases in this paper as they all have fully turbulent flow.

The CODISC process begins with a flow solution for a baseline configuration. From this flow solution and the baseline CFD grid, the extraction module obtains surface geometry, pressures, and skin-friction data at the design stations utilized by CDISC. The original extraction module has been modified to also provide the global force and moment information required by the SOUP module for optimization.

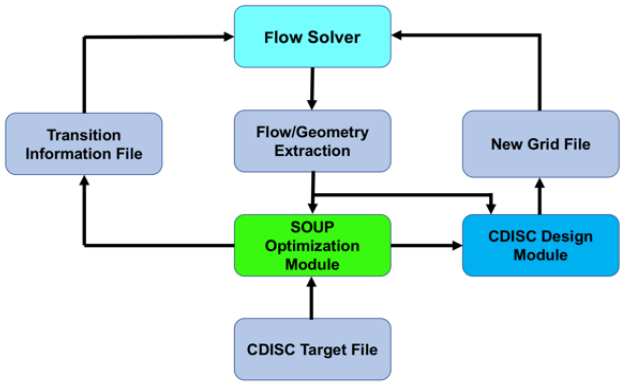

Figure 2. Flow chart of the CODISC design system.

A. Optimization Module (SOUP)

The information from the extraction module is passed to the SOUP code, along with the CDISC target file, where it is used to drive the adjustment of selected input parameters for some of the CDISC flow constraints. In addition to the global force and moment information, local values of lift and drag at each design station are also computed from the surface geometry, pressure, and skin-friction data. These local forces could allow for the independent adjustment of the optimization parameters at each design station. To date, however, this option has not provided consistent results and is therefore not used in the test cases presented in the Results section. Two possible reasons for this inconsistency are currently being examined. The first is that there is insufficient grid resolution for accurate local drag values. The second is that the flow at a design station is not independent of changes at nearby stations, thus an improvement at one station could degrade the flow nearby, possibly leading to an increase in total drag.

The SOUP module is called before CDISC in each CODISC design cycle; however, the optimization variable is only updated if the current lift coefficient is within a prescribed variation around the design lift coefficient (typically, ± 0.5 per cent), and the current design cycle is beyond a user-specified starting point. An option is available in SOUP to adjust the desired section lift coefficients in the target file to move the total lift toward the design value without altering the configuration angle of attack. This option was used in all of the 3-D cases presented in this paper. An alternate approach would be to use a lift matching in the flow solver itself, which was done for the 2-D examples.

The CODISC process continues until one of the following conditions are met: 1) a normal minimum is found, where the drag has increased above a previous minimum value by a specified amount; or 2) a flat minimum is detected, where the drag has remained within a specified variation for a given number of optimization cycles, varying from 10-

40, depending on the flow solver. For both of these stopping criteria, the lift also must have remained within its specified tolerance for the same number of cycles. The specified values for the normal and flat minimums should be large enough to avoid early termination due to any noise in the drag versus design cycle data.

While the objective function in CODISC is usually the minimization of drag, a unique feature in the SOUP module is that it can be used to adjust the midchord gradient variable (V_1, see figure 3) in the primary flow constraint to obtain the best fit of the target pressures to the original analysis pressures. This option cycles only through the SOUP and CDISC modules in CODISC, adjusting the V_1 variable at each station until the difference between the target and analysis pressure distributions is a minimum. This provides initial V_1 values to the design process that allow the actual CDISC design to quickly match the target pressures and desired lift coefficients, thus allowing CODISC to start the optimization phase sooner. Also, when starting from a baseline that already has good performance, it provides a check on how suitable the target pressure architecture is for the configuration. Note that these initial pressure distributions will evolve as the design rule is applied to the current analysis pressures, which will change as the design progresses and geometry constraints are also applied. Finally, the initial best-fit values provide a spanwise distribution of the V_1 parameter to be scaled or shifted by a single optimization variable driven by total drag.

B. Design Module (CDISC)

As mentioned earlier, CDISC automatically generates the target pressures that it tries to match from flow constraints and the current analysis pressures. A single flow constraint was used to create the basic target pressure architecture for all of the design cases in this paper and it is the one adjusted by SOUP during optimization runs. Though originally created for natural laminar flow (NLF) design at supersonic cruise conditions [11], it has since been modified for use with laminar and turbulent designs at transonic as well as supersonic speeds [12-14]. The parameterization for this constraint for a typical transonic NLF case is shown in figure 3. In this figure, X_{ca} marks the end of the rapid acceleration used for crossflow (CF) attenuation and the beginning of the midchord pressure gradient region (V_1) used to control Tollmein-Schlichting (TS) mode growth. The X_{tr} variable is the desired transition location. A mild adverse gradient is prescribed aft of X_{tr} to reduce the shock strength at the termination of the pressure rooftop, X_{shk}.

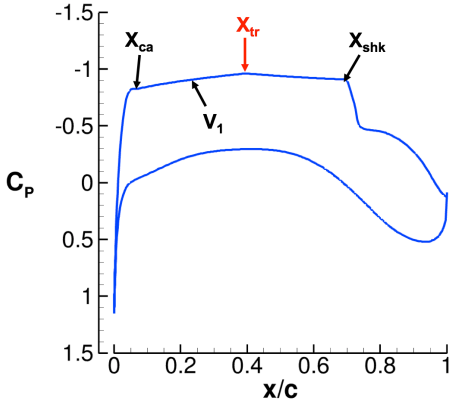

Figure 3. Target pressure architecture for laminar flow.

For NLF optimization, X_{ca} and X_{shk} are set based on empirical design rules, while X_{tr} is adjusted based on the change in drag from the previous design cycle. As the transition location is adjusted, the midchord gradient parameter needs to be modified as well to ensure that the TS growth envelope meets the critical N-factor limit at X_{tr}. Ideally, the required gradient value would be iteratively determined using a boundary layer stability analysis code, but the time needed to do this would be prohibitive. Instead, an empirically-derived relationship that sets the value of the gradient based on the chord Reynolds number, desired transition location, and TS critical N-factor has been built into CDISC to automatically estimate the required gradient value.

An assessment of the accuracy of this gradient estimation algorithm is shown in figure 4. The actual X_{tr} values were computed using the LASTRAC boundary layer stability analysis code [15] and the target pressures generated from the flow constraint for values of chord Reynolds number of 20, 30, and 40 million, transition x/c locations from 0.3 to 0.6, and a fixed TS critical N-factor of 10. In the primary region of interest, x/c = 0.4 - 0.6, the predicted and actual values of X_{tr} are fairly close, usually within 0.05c, indicating that the V_1 value from the algorithm gives the desired TS growth rate. During design, the transition location is restricted to be at least 0.1c ahead of the shock location to avoid the risk of laminar separation at the shock.

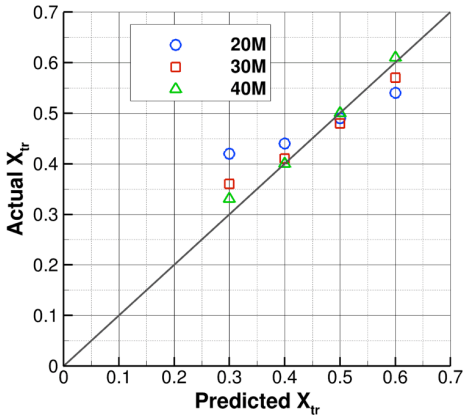

Figure 4. Assessment of the midchord gradient (V_1) estimation algorithm.

A transonic NLF optimization would ideally involve a trade between the extent of laminar flow, and the corresponding reduction in skin-friction and profile drags, with a potential increase in wave drag due to the midchord gradient required to suppress TS growth. An NLF design using this approach was reported in [14] that verified the utility of the V_1 estimation algorithm, but subsequent assessment of the local-drag optimization capability suggested that it was not fully functional. Work continues on developing an alternative local-drag option that focuses specifically on wave drag. A description and preliminary assessment of his new option is included in the Transonic wing subsection for turbulent flow design, with a goal of future application for NLF optimization.

For turbulent flow cases, X_{tr} is moved to be coincident with X_{shk}, with that location based on a blending of the current analysis shock location and a prescribed position based on a function of Mach number. This method has added stability to the design process and is a significant improvement over the previous versions of CDISC. This design rule was initially developed using 2-D airfoil optimization cases, then modified to account for the sweep and taper present in a 3-D wing. It may require further modification for root and tip effects, but these are not included in the present design rule. The midchord gradient variable V_1 is optimized during the turbulent flow design, with the resulting pressure rooftop typically having a slightly concave adverse gradient terminating in a weak shock (see figure 5). Several unpublished applications of this constraint for turbulent design, without the SOUP optimization, produced significant drag reductions at the design point with good off-design performance; however, those designs were started from baselines with rather poor performance. The design cases in this paper generally start from good baselines, and the results will be compared with ones from other optimization methods when available.

For the transonic cases included in the Results section, an additional flow constraint is used to set the pitching moment at each design station. Based on SOUP optimization runs for this constraint using the 2-D MSES code, it was determined that minimum drag occurred for the candidate airfoil when the pitching moment was adjusted to give a skin friction value of 0.00005 at the trailing edge. The pitching moment constraint in CDISC was therefore modified to automatically adjust the moment value to try to obtain this value. While this approach may need further evaluation to show that it can be used for other configurations, codes, and conditions, so far it has produced very reasonable airfoils with good performance.

A similar process was used to develop rules for setting input parameters for other flow and geometry constraints. In many cases, the default values are coded into CDISC and are triggered by special constraint input variable values. In an effort to make the setup of the initial target file easier for users, an auxiliary code has been developed to automatically create a target file from the original flow and geometry information with a typical set of flow and geometry constraints, using the new recommended values.

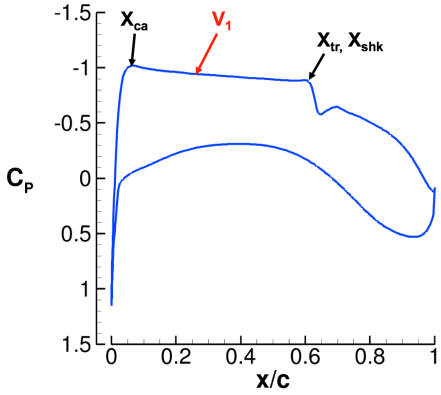

Figure 5. Target pressure architecture for turbulent flow.

III. Results

Three test cases are included below to illustrate some of the capabilities of the new CODISC design system. In each case, the flow solver was selected to give as quick a turnaround as possible, based on the case objectives and speed regime. For the transonic cases, a couple of options for improving off-design performance without having to do formal multipoint optimization are explored. As mentioned before, the designs all use the turbulent design approach.

A. Supersonic Design

The first set of design cases use the CART3D Euler flow solver [9] in the CODISC process to try to improve the cruise performance of a generic supersonic transport configuration [11]. This flow solver was selected in part because it is very fast and the absence of viscous effects should have minimal impact at the design condition. In addition, the baseline configuration was designed using the adjoint optimization capability in CART3D by an experienced user (Dr. Matthias Wintzer). The configuration served as a baseline in a cooperative NLF design effort between NASA and the Japanese aerospace agency, JAXA, and is referred to as the NASA-JAXA Wing Body (NJWB). A turbulent CODISC design was previously performed on this configuration as reported in [13], but a different flow constraint was used. The design has been repeated here to assess if a single flow constraint can be used, regardless of the type of design (laminar or turbulent) or speed regime.

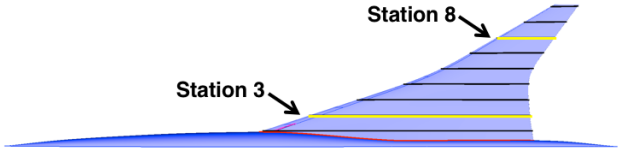

Figure 6. NJWB planform with design stations.

A planform view of this configuration is shown in figure 6, with the design stations marked as black or yellow lines. The design conditions are Mach = 1.6 and a lift coefficient of 0.10. The CDISC design retains the spanwise lift, maximum thickness, and leading-edge radius distributions of the baseline, while using the flow constraint to create the target pressures from the current analysis pressures. This case should provide a good challenge to the CODISC method as it is already highly refined having previously been optimized. It will also allow the first check on the target pressure architecture for this flow constraint as it has not been used for supersonic turbulent flow design.

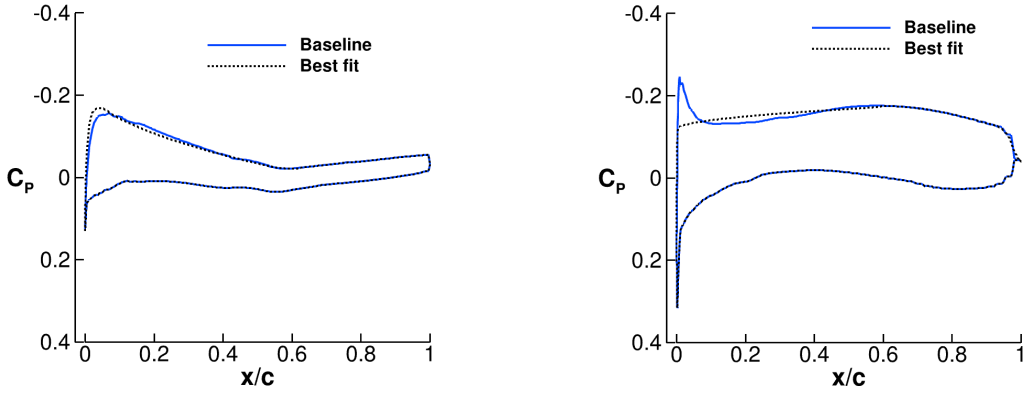

a) Station 3 **b) Station 8**

Figure 7. Comparison of best-fit target pressures and baseline analysis pressures

The best-fit process was applied to the original analysis pressures, with the results shown in figure 7 for design stations 3 and 8, indicated on figure 6. In general, there is a good match between the best-fit target and the baseline analysis pressures. The targets have a slightly higher peak inboard, but have removed the leading-edge peak completely at the outboard station. If this outboard peak is a key to good performance, the CODISC design is not likely to improve upon the baseline drag level. The best-fit V_1 values at all design stations across the semispan are shown in figure 8. The distribution is fairly linear in the middle of the wing as shown by the blue line in the figure, with some flattening at both the root and tip. For the optimization case in this paper, a linearly varying increment with no change at the tip will be added to these best-fit initial values. If the baseline was not a well-designed starting point,

the results in figure 8 suggest that a linear initial distribution might be a good starting point. Ideally, if the local drag optimization was working well, it could be used to vary the shape from any initial distribution.

A basic CDISC design (no optimization) using the best-fit targets was run and the convergence results for lift and drag are shown in figures 9a and 9b, respectively. While no optimization was used in this design, the SOUP module is still run to adjust the section lift coefficients to try to match the original baseline total lift and to apply the stopping criteria. A flat drag minimum was reached after 78 design cycles at a value of 0.00383, or about a 1.1 count drag reduction relative to the baseline (recall that the case is inviscid, thus the fairly low cruise-drag values). The lift adjustment procedure in SOUP worked very well, matching the baseline lift coefficient within about 0.1 percent. Considering that the baseline itself is an optimized configuration, the drag reduction from the design is significant and indicates that the best-fit approach to defining initial target pressures gives a good starting point.

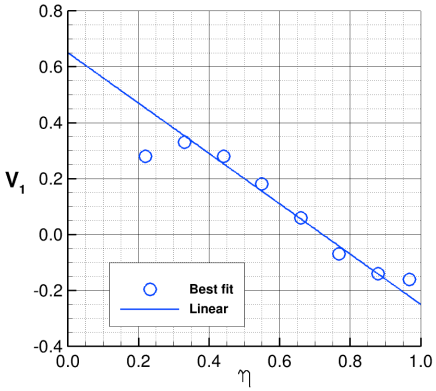

Figure 8. Spanwise distribution of V_1 from best-fit procedure.

In order to test the robustness of the flow constraint and design procedure, the case was repeated starting from a version of the baseline that had the camber and twist removed from the wing. The convergence histories for this case are shown in figure 10. The initial analysis for this case was run at the same angle of attack as the previous case, which resulted in significantly higher initial lift and drag coefficients, 0.124 and 0.00663, respectively, well above the y-axis values in figure 10. As the initial pressure distributions were considerably different from the original best-fit targets, especially towards the wingtip, the design took longer to match the design lift and for the drag to settle out. After 123 design cycles, a flat drag minimum was reached at 0.00382, within 0.1 counts of the value starting from the original baseline. The number of cycles required was about 50 percent more than for the previous design that started from the original baseline. This result gives a preliminary indication that the CODISC process is fairly independent of the starting point, thus putting less of a requirement for refinement on an initial configuration in the design process.

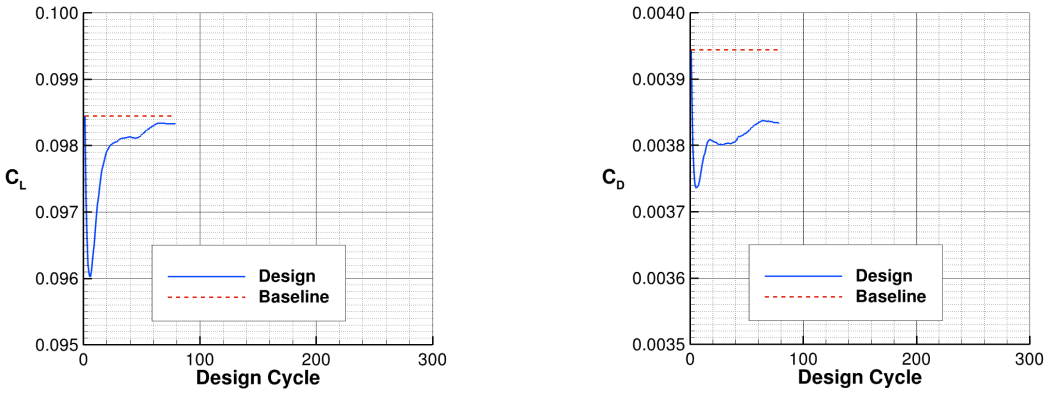

a) Lift **b) Drag**

Figure 9. Convergence histories for baseline to best fit CDISC-only design.

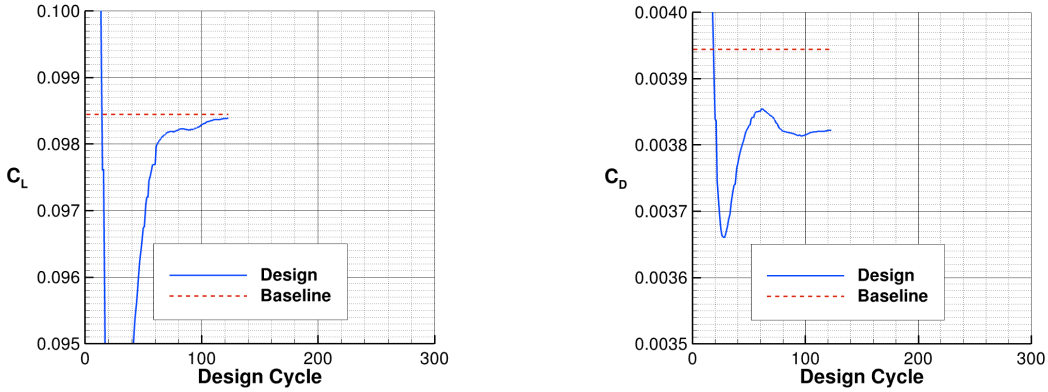

a) Lift **b) Drag**

Figure 10. Convergence histories for best fit CDISC-only design starting from baseline with wing camber and twist removed.

While both of the CDISC designs above did use the CODISC optimization capability in the sense of starting from the best-fit targets, one of the goals of the CODISC development is to see if a good CDISC design can be improved by automatically varying an input parameter, such as V_1. To examine the effectiveness of CODISC in this regard, an optimization run was started from the final cycle from the CDISC design of the original baseline. The objective function was total drag and the design variable was the magnitude of a linear V_1 increment applied to the original best-fit V_1 distribution. The final convergence histories are plotted in figure 11. The target lift value is well-matched and a normal minimum was found at cycle 253, with a minimum drag coefficient of 0.00378. This represents a further drag reduction of 0.5 counts below the CDISC-only design and a reduction relative to the baseline of 1.6 counts, or 4 percent of the total (inviscid) drag. The final V_1 distribution in figure 12 shows that the value at the wing root increased by about 0.14, with the change linearly decreasing to zero at the wingtip.

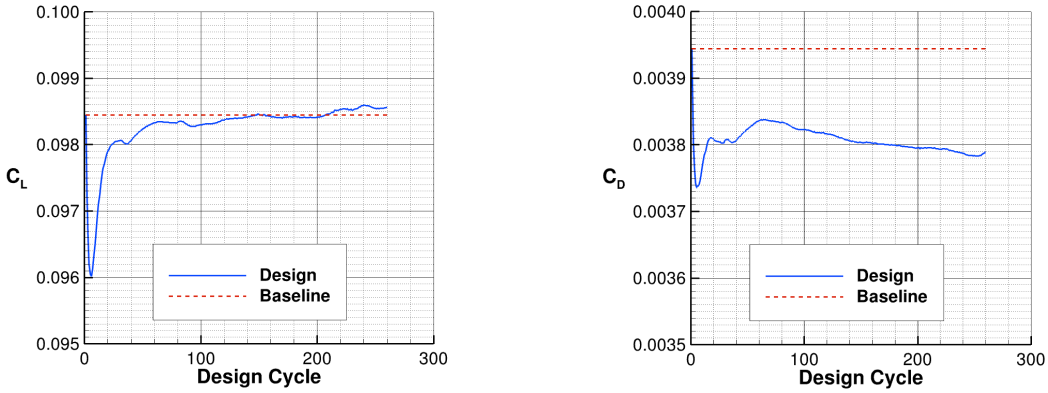

a) Lift **b) Drag**

Figure 11. Convergence histories for CODISC optimization starting from CDISC design of the original baseline.

The CODISC design took a little more than twice the number of design cycles needed for the original CDISC-only design, well within the desired efficiency goal. It should be noted that the allowed changes for CDISC as well as SOUP were intentionally set to fairly small values to ensure stability in this initial evaluation of the CODISC process, resulting in more design cycles than the typical 30-50 for a CDISC design. It is anticipated that larger changes can be used, but that the ratio of CODISC to CDISC-only cycles would be similar to this case.

To summarize the results for the supersonic design, the use of the flow constraint with the best-fit option in SOUP produced very reasonable target pressures for a CDISC-only design that provided a drag reduction relative to the baseline. A CODISC optimization, started from the CDISC-only design, was able to produce further improvement in the drag level and only required about twice as many additional design cycles, thus meeting the original objectives of effectiveness, efficiency, and ease of use.

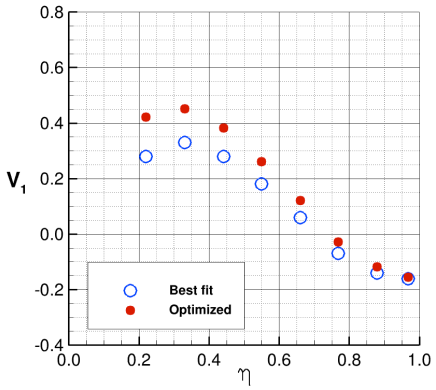

Figure 12. Spanwise distribution of V_1 from CODISC optimization and best fit procedure.

B. Transonic Airfoil Design

Historically, the primary application of CDISC has been in the area of transonic design. Most commercial transports and business aircraft cruise at transonic speeds, so any improvements in performance at these conditions could result in significant fuel savings for airlines and corporate jet operators. Though the focus in this paper is on the turbulent flow option with the primary flow constraint, the NLF design option in that constraint could provide even more drag reduction if the design could be practically manufactured and maintained.

Recently, a series of 2-D CODISC optimizations were made for both laminar and turbulent flow cases [13]. The runs were started from the D0 airfoil that had been used in a previous airfoil design study by Wu [16]. The results from CODISC in the recent study showed that it could achieve drag reductions at the design point similar to ones from an adjoint-based optimization method used by Wu. Analysis at off-design conditions, however, indicated that both the CDISC-only design and CODISC optimization airfoils (as well as the baseline D0 airfoil) demonstrated a somewhat pronounced drag "bucket" near the design point. While this type of undesirable behavior is usually addressed by doing formal multipoint optimization, it was decided to see if the off-design penalty could be mitigated by the use of CDISC flow and/or geometry constraints. If this approach proves successful, the added expense and time required for multipoint design could be reduced or eliminated.

In order to reduce the time required to do the optimizations, as well as compute drag polars and dragrise curves for assessing off-design performance, the MSES 2-D flow solver [8] was chosen. The code is an Euler method with an interactive boundary layer used to compute viscous effects. While the Newton solver used by the code is very efficient, it is also fairly sensitive, especially when run in the lift-matching mode that was used in this study. This required the use of fairly small design changes to keep the design process stable, resulting in the need for hundreds of design cycles, though the design time was still in terms of minutes due to the speed of the flow solver.

The design condition for all of the following optimization cases was a Mach number of 0.76, a lift coefficient of 0.7, and a chord Reynolds number of 30 million. A new CDISC flow constraint that sets the pitching moment to an "optimal" value was also included in the designs below. This constraint was developed by using SOUP to adjust the pitching moment until a drag minimum was found. Over several different test conditions, the drag minimum correlated with a skin friction coefficient value of 0.00005 at the trailing edge of the upper surface. This new design rule was added to the pitching-moment constraint in CDISC so that SOUP, which can only adjust one constraint per run at this time, was free to work on the primary flow constraint. Further assessment of the optimum pitching moment criteria, especially at off-design conditions and with other flow solvers, is needed to confirm that it can be generally applied.

The first case is a basic CODISC optimization with no additional constraints used to try to improve the off-design performance. As with the supersonic designs, the initial V_1 value was set using the best-fit option in SOUP. The resulting drag convergence history is shown in figure 13. The lift convergence plot is omitted as the flow solver matches the desired lift at every design cycle. The initial CDISC-only design reaches a flat minimum at cycle 188,

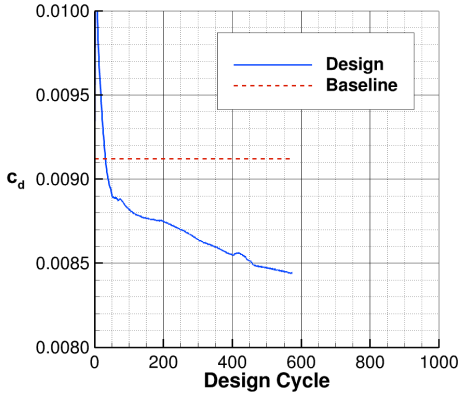

Figure 13. Basic CODISC optimization of D0 airfoil.

with a drag reduction of 3.6 counts relative to the baseline value of 0.00912. At this point, SOUP begins to adjust the V_1 parameter, continuing until a normal drag minimum is found at cycle 570, or about 2x more additional cycles than the CDISC-only portion of the design. The final minimum drag is 0.00844, a reduction of 6.8 counts or about 7 percent relative to the baseline, which is nearly identical to that obtained by Wu with optimization. Thus, the use of SOUP was able to almost double the drag benefit obtained using only CDISC.

The primary cause of poor off-design performance at lift coefficients or Mach numbers lower than the design values is the collapse of the supercritical rooftop leading to an early shock, followed by a reexpansion to a second, sometimes stronger, shock. Two constraints are proposed to address this issue. The first is a geometry constraint to limit curvature variations in the supercritical zone, with a specific goal of limiting any flow re-expansion to weaken any secondary shocks. The second constraint is a flow constraint that locally limits the adverse pressure gradient in the rooftop region based on the slope of the airfoil upper surface geometry. Prior experience has shown that better multipoint performance can be obtained using less adverse rooftop gradients, but this usually means a stronger shock and more wave drag is present at the design condition.

To test these new constraints, 3 additional CODISC optimization runs were made: one with each constraint applied separately, and one with both constraints active. The resulting drag convergence histories are shown in figures 14 – 16. All of these runs finished the CDISC-only portion, indicated by the fairly flat drag region between cycles 150 and 190, slightly earlier than the original optimization run. The two cases that included the adverse rooftop constraint (figures 15 and 16) continued running to almost 1000 cycles, though the additional drag reductions in the final 500 or so cycles were minimal. The occasional spikes occurring in the plots were the result of the MSES flow solver not fully converging for that design cycle. These runs required modifications to the SOUP module to increase its robustness and allow the process to continue past this type of transient behavior. The two runs with the individual constraints had minimums that were within about 1 count of the minimum for the original optimization. The double-constraint run minimum was slightly higher, but, in general, all of the constraint runs had a fairly small impact on the drag at the cruise condition.

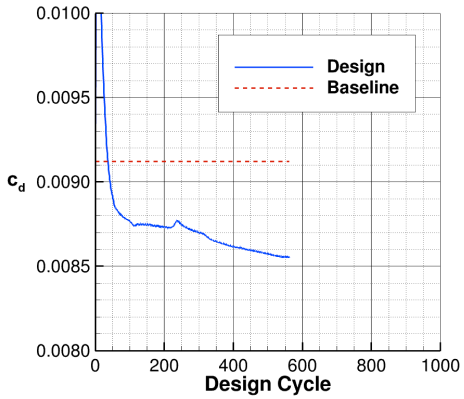

Figure 14. CODISC optimization of D0 airfoil with curvature constraint.

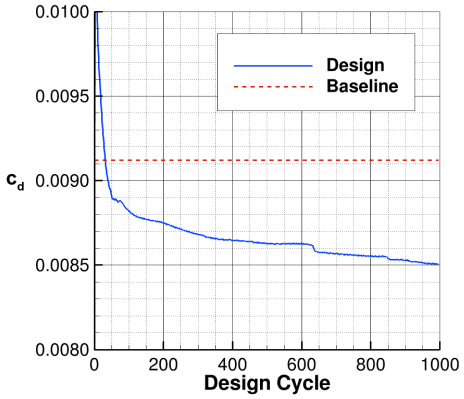

Figure 15. CODISC optimization of D0 airfoil with rooftop gradient constraint.

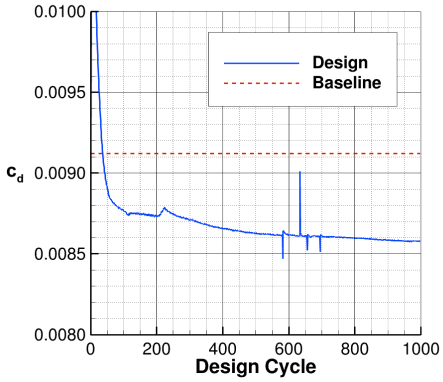

Figure 16. CODISC optimization of D0 airfoil with both curvature and rooftop gradient constraints.

In order to evaluate off-design benefits, drag-polar and dragrise cases were run for the baseline and all four optimization runs, with the results plotted in figures 17 and 18. In figure 17, it can be seen that, not only does the baseline D0 airfoil have a drag bucket, but the bottom of the bucket occurs well ahead of the design lift coefficient of 0.7. The basic optimization run realigns the drag bucket with the design lift coefficient, pushing the final drag rise to higher lift values, but it does have a lift drag creep peak near $c_l = 0.6$ that is nearly twice as high as for the baseline. Adding the curvature constraint softens this peak somewhat, but the two runs with the gradient constraint do the best job of reducing the magnitude and abruptness of the lift drag creep peak.

A similar story can be seen in the drag rise curves in figure 18, where the baseline bucket again occurs earlier than the design point of M = 0.76, and there is an extensive drag creep peak at lower Mach numbers. Though the basic optimization creates a fairly narrow drag bucket, which is not desirable, it does increase the dragrise Mach number and, in general, has better performance than the baseline at lower speeds. In this figure, all of the constraint cases improve upon the performance of both the baseline and basic optimization. While the addition of the constraints has not eliminated drag buckets, and the constraint values may need further refinement, these results suggest that the constraint approach may be an effective and efficient way of reducing the need for multipoint design. Further study will be needed to see what, if any, modifications will be needed for application to wings where airfoils shapes can vary significantly from root to tip.

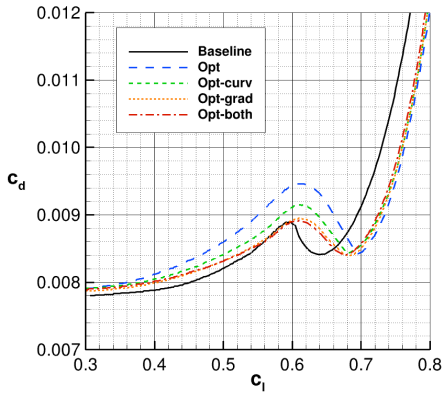

Figure 17. Drag polars at M = 0.76.

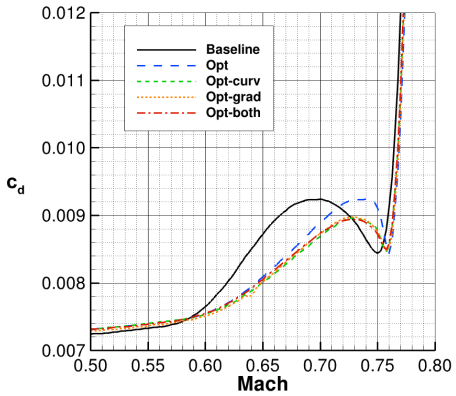

Figure 18. Dragrise curves at $c_l = 0.7$.

C. Transonic Wing Design

Based on the guidelines and constraints developed during the supersonic wing and transonic airfoil design studies, a series of transonic wing optimization cases will be attempted. At these conditions, it is essential to include viscous effects, so the designs will be done using the USM3D flow solver [10]. This code solves the Navier-Stokes equations on a tetrahedral unstructured grid and, for all of the cases shown, will use the Spalart-Allmaras turbulence model. The baseline configuration is the Common Research Model (CRM) [17] run at a Mach number of 0.85, lift coefficient of 0.5, and Reynolds number of 30 million, based on a mean aerodynamic chord of 275.8 inches. A planform view of the CRM with the design stations indicated by black and red lines is shown in figure 19.

The CRM has been used in a number of previous design studies, including numerical optimization [18-20] as well as CDISC [12] and some earlier CODISC applications [13,14]. In the current study, the baseline lift coefficient and maximum thickness-to-chord ratio at each design station will be maintained, under the assumption that, in actual aircraft design, these values are determined more by structural limitations than by aerodynamic performance. Holding the lift coefficients constant eliminates reducing induced drag by making the spanload more elliptical. Profile and skin-friction drag reductions due to decreasing the airfoil thicknesses are also prevented. Thus, the primary source of drag improvement will be wave drag reduction, with perhaps some secondary profile drag benefits, from reducing shock strength via airfoil shaping.

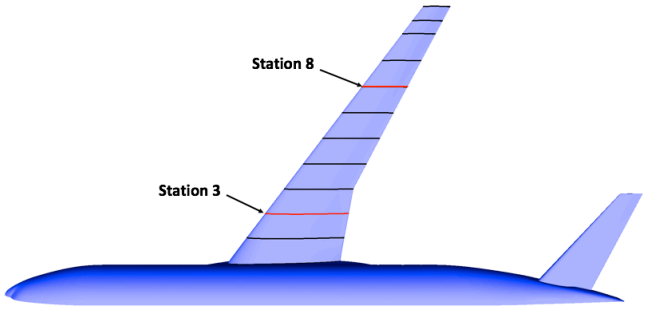

Figure 19. Planform view of the CRM baseline with wing design stations indicated by black and red lines.

Three cases will be used to illustrate the CODISC methodology. The first is a design to the initial target pressures developed using the best-fit option in CODISC, similar to the first supersonic design. The second case is the same as the first, but with the new optimum pitching-moment constraint added. During the optimization phase for both of these cases, the design variable is a linear increment in V_1, added to the initial best-fit distribution and driven by total aircraft drag. The third case will investigate a new approach to determining an optimum spanwise distribution of V_1. As noted earlier, the local drag option in the SOUP module was not providing consistent enough results for use in making separate design variable changes at each station. Therefore, an alternative approach, focusing just on wave drag, has been developed. For this option, the V_1 value at each station will be adjusted to bring the component of shock Mach number normal to the shock (M_{1n}) at that station below a target value. A target value of $M_{1n} = 1.0$ was selected for this initial trial.

The best-fit results for the initial target pressures for all three cases at design stations 3 and 8 (see figure 19) are shown in figure 20. The best-fit target pressures are an extremely good match at both stations, better than the fitting for the supersonic case. The best-fit distribution of V_1 across the wingspan is shown in figure 21 and, as with the supersonic wing design, is fairly linear and decreasing from root to tip.

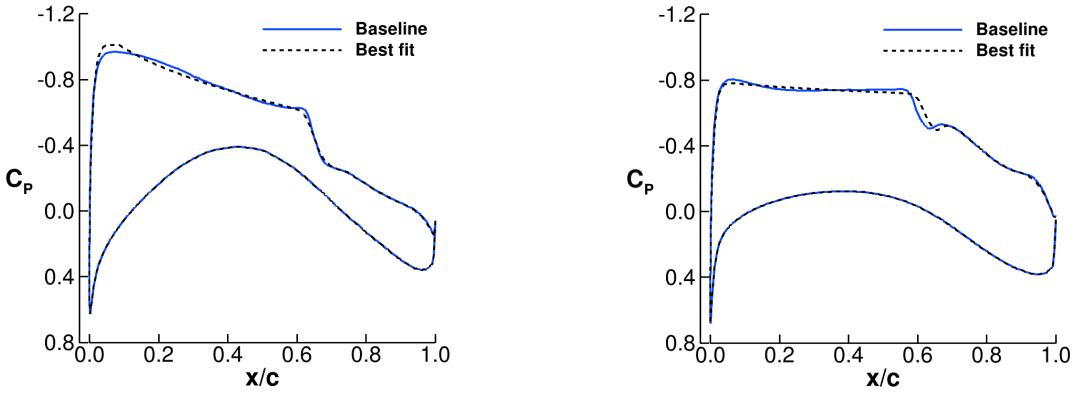

a) Station 3 **b) Station 8**

Figure 20. Best-fit pressure distributions for the CRM.

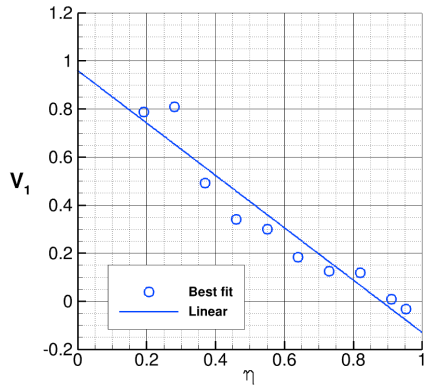

Figure 21. Spanwise best-fit distribution of V_1 for the CRM.

The lift and drag convergence histories for the basic optimization without the pitching-moment constraint are shown in figures 22a and 22b, respectively. As with the supersonic cases, the lift-matching option in SOUP was used to adjust the wing section lift coefficients to drive the total aircraft lift coefficient to match the baseline value of 0.5. The lift and drag meet the criteria to end the CDISC-only design and begin the optimization process at cycle 31, reaching a drag coefficient of 0.02345, corresponding to a reduction of 1.2 counts from the baseline value of 0.02357. While this is not a dramatic reduction, it does indicate that the best-fit option for determining the initial target pressure architecture is a good approach when starting from a well-designed baseline. As noted earlier, a side benefit of this approach is that the initial CDISC portion of the design tends to converge quickly, allowing the optimization to start earlier. The baseline run (not shown), converged to a specified lift coefficient, required the same number of flow solver iterations as 56 design cycles, so the CDISC-only design took just over half as much time as the original analysis. The main reason for the rapid design time is that CDISC uses prescribed sensitivity derivatives in altering the geometry to match the current target pressures, so that highly-converged solutions or adjoint solver runs are not required. For these cases, only 500 flow iterations beyond the previous solution restart are needed to provide sufficient accuracy to advance the design at each cycle.

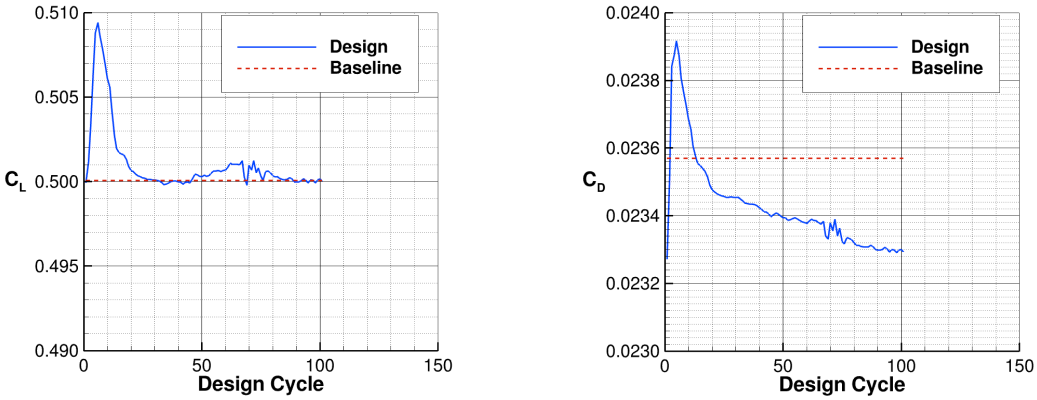

a) Lift **b) Drag**

Figure 22. Convergence histories for basic CODISC optimization of the CRM.

The optimization continued to a total of 100 design cycles, with the drag dropping another 1.5 counts to a final drag coefficient of 0.02330. The initial best-fit and final optimization V_1 distributions are shown in figure 23. The optimization increased the V_1 values across the span using the linear increment approach, but note that the value at the innermost two design stations hit the limiting value of 1. This case shows that CODISC is effective at improving a CDISC design that was already an improvement from a good baseline. As the total CDISC plus CODISC time was approximately twice the time required for the initial baseline, it also meets the efficiency goal laid out at the beginning of the study.

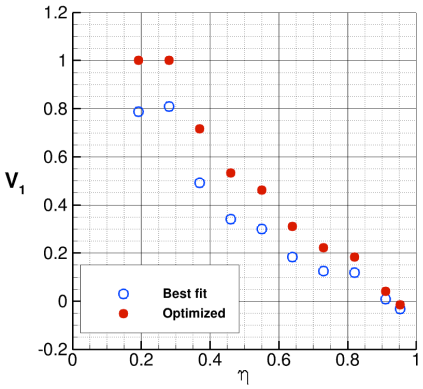

Figure 23. Spanwise best-fit and optimized distributions of V_1 for the CRM.

For the second design case, the constraint that adjusts pitching-moment based on the value of the skin-friction coefficient at the trailing edge of the airfoil upper surface was added. As mentioned in the transonic airfoil design study, this constraint does not require the SOUP optimization module, but works according to a design rule developed from CODISC runs. As skin-friction values can be slow to respond to design changes, and also may vary between flow solvers, upper and lower limits on c_m are internally set as a function of c_l (-0.11 and -0.22 times c_l, respectively) to help avoid unrealistic values as the design progresses.

The convergence histories for this case are plotted in figure 24. The CDISC-only portion was converged by design cycle 28, again requiring about half the time of the baseline analysis. The drag reduction at this point, relative to the baseline, is 1.7 counts, or about 0.5 counts lower drag than the first case at the end of the CDISC design. At the end of 100 design cycles, the drag had dropped an additional 1.4 counts, for a total of 3.1 counts less than the baseline. The final spanwise distribution of V_1 is shown in figure 25 and is nearly identical to the one from the basic optimization (figure 23). These results suggest that the "optimum" pitching moment constraint should be included in future designs, but it should be noted that no penalty relative to trim drag has been included. The final values of aircraft C_m for the baseline, basic optimization, and optimization with c_m constraint are -0.059, -0.063, and -0.070. Perhaps the speed of the CODISC design system would allow this information to get into the overall aircraft design process early enough that the change could be absorbed without penalty.

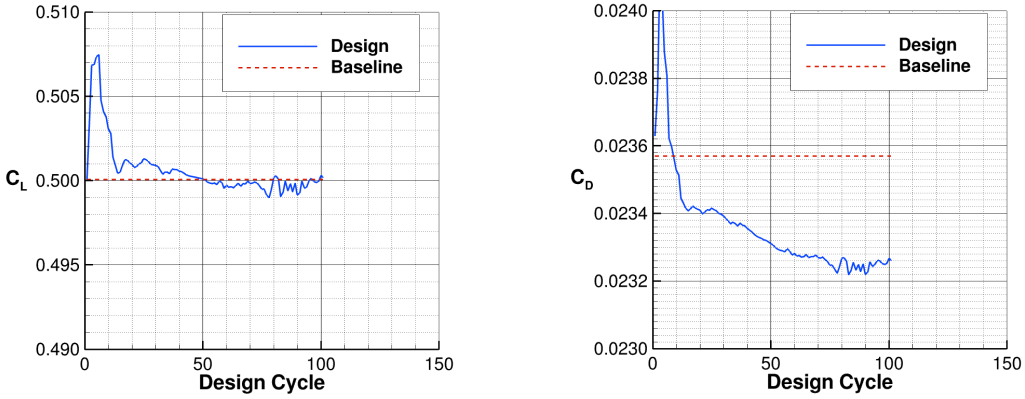

a) Lift **b) Drag**

Figure 24. Convergence histories for CODISC optimization of the CRM with c_m modification.

For the two previous cases, a linear increment in V_1, with no change at the wingtip, was used as the design variable. This was selected based on several forms tried in the supersonic design study. While it was effective at providing further drag reductions relative to a CDISC-only design at both supersonic and transonic speeds, there is not a strong reason for limiting the changes for stations on the outboard portion of the transonic wing. As the design problem has been set up with a focus on wave drag reduction, ideally the V_1 parameter at each design station should be adjusted individually to reduce the strengths of any shocks present. A modification has been made to SOUP to evaluate this concept, with the objective function no longer total drag, but rather the value of the Mach number upstream and normal to the shock (M_{1n}). As implemented, the design variable V_1 will be increased at each design station, if needed, until M_{1n} at that station is less than 1.0.

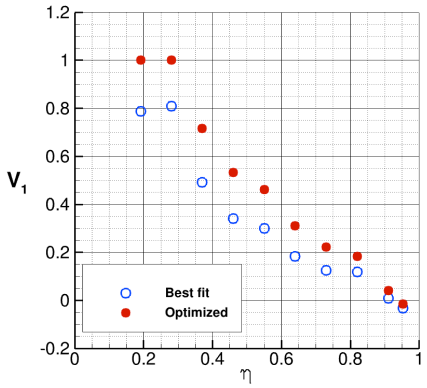

Figure 25. Spanwise best-fit and optimized with c_m modification distributions of V_1 for the CRM.

In order to provide the value of M_{1n}, a procedure is used to compute both the chordwise location and Mach number just upstream of the shock based on the pressure gradient. Because the shock extracted from the CFD solution can be rounded due to numerical dissipation, grid density, etc., these values can lack accuracy and consistency, especially for the weakened shocks that are the goal of the design. Fortunately, the wave drag is proportional to $(M_{1n} - 1)^4$, so the final weak shocks do not contribute much to the total drag anyway.

A partial loop through CODISC, similar to the best-fit procedure, was set up to test this algorithm. In the loop, SOUP continues adjusting the V_1 parameter at each station to drive the M_{1n} values derived from the target pressures from CDISC below a value of 1.0 at every station. Plots of the spanwise distribution of M_{1n} from this process, along with the baseline values, are shown in figure 26. One observation is that the M_{1n} values for the baseline are fairly small, implying that there is not a lot of wave drag to eliminate, thus the limited reductions seen in the first two cases. The higher Mach numbers inboard would have been affected by the linear V_1 increment. The outboard region with M_{1n} greater than 1.0 would not have been significantly changed by SOUP, though the initial best-fit targets for CDISC did provide some weakening of the shocks. The M_{1n} values from the final target pressures were all below the limit, suggesting that the new optimization driver will be effective.

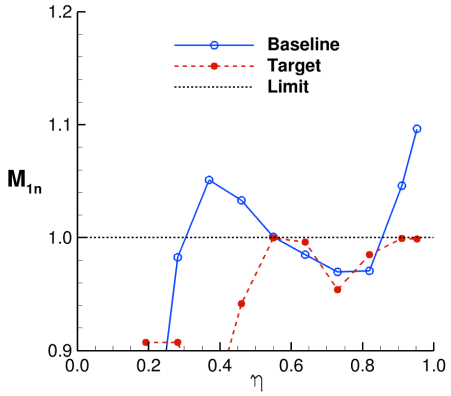

Figure 26. Spanwise distribution of M_{1n} for the baseline and new objective function evaluation procedure.

Figure 27 shows the convergence histories for this case, with the flattening of both the lift and drag curves near cycle 30 indicating the end of the CDISC-only portion of the design, giving the same drag coefficient (0.02345) as the first case, as expected. At this point, the SOUP module begins checking the M_{1n} value at each station and increasing the V_1 value if M_{1n} is greater than 1.0. A minimum drag value of 0.02336 occurred at cycle 95, thus giving a total drag reduction of 2.1 counts relative to the baseline. Figure 28 shows the final spanwise distribution of the V_1 parameter, which has lost some of its linearity, especially near the tip. The reason for this can be seen in the spanwise distributions of M_{1n} shown in figure 29. The new optimization driver has increased V_1 at the last two stations to reduce the M_{1n} values there, where the previous approach with the linear V_1 increment would not have had much effect. However, the M_{1n} value at the station near $\eta = 0.37$ was not reduced as hoped, perhaps explaining why this case had the least drag reduction of the three wing designs. Figure 28 indicates that the V_1 value did increase as expected, but it is not clear at this time why it did not produce the desired effect. Also, in examining the design pressures at the station near $\eta = 0.46$ (not shown), even though the M_{1n} value, which is based on the target pressures, was below 1.0, the design pressures missed the targets near the shock, having a higher Mach number.

While the M_{1n} driver currently operates only to drive values below the target value of 1.0, it might be worth investigating having it also increase lower Mach numbers up to the target value by lowering V_1 values. Limiting the adverse rooftop gradient specified by V_1 was shown to have a beneficial effect at off-design conditions in the airfoil studies and this might be a way of imposing only as much rooftop pressure gradient as needed to eliminate wave drag.

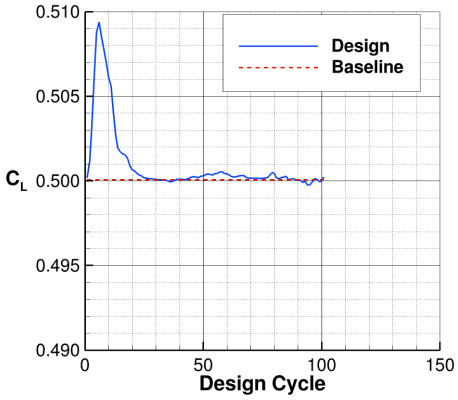

a) Lift

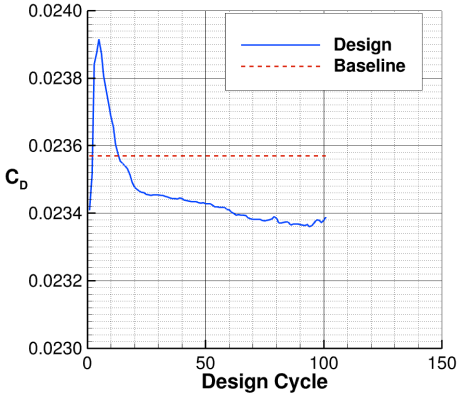

b) Drag

Figure 27. Convergence histories for CODISC optimization using M_{1n} driver.

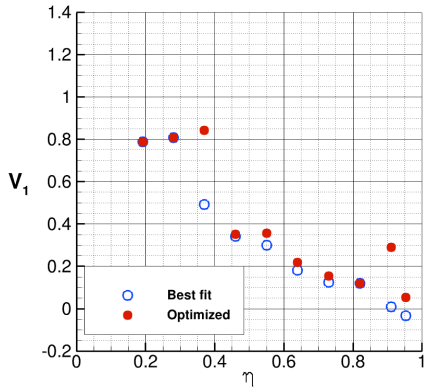

Figure 28. Spanwise distribution of V1 for CODISC optimization using M_{1n} driver.

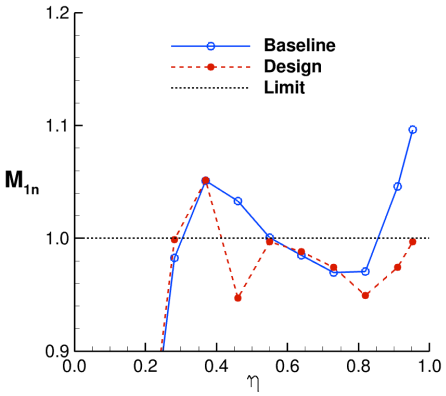

Figure 29. Spanwise distribution of M1n for CODISC optimization using M1n driver.

To summarize the results from the transonic wing design cases, all cases produced drag reductions relative to the baseline at the end of the CDISC-only design portions of the CODISC runs. This indicates that the flow constraint creates a reasonable target pressure architecture and that the best-fit approach is a good way of determining the initial V_1 values for that constraint. The additional CODISC optimization cycles always gave further drag reduction and only required about twice as many design cycles as the CDISC-only design. The run with the optimum c_m constraint produced the lowest drag value of the runs shown. Finally, the new optimization driver was effective at reducing the total drag by using local adjustments to M_{1n} to reduce wave drag.

IV. Concluding Remarks

The test cases shown in this report indicate that the CODISC design system meets the goals set at the beginning of the study based on the three Es: effectiveness, efficiency, and ease of use. In order to provide a rigorous test of the effectiveness of CODISC, the baseline starting points were chosen as well-designed configurations. For both the supersonic and transonic wing design cases, CFD-based optimization codes were used to develop the baseline geometries. For each of the three test cases, the basic CDISC design was able to improve the performance of the baseline. The success of CDISC was due in large part to the best-fit process developed for determining initial values of the optimization variable for a baseline with good performance. Subsequent CODISC optimizations, starting from the CDISC-only design, were always able to provide further drag reductions, comparable to numerical optimization

results when they were available. The CODISC optimization process was also used to create a new CDISC flow constraint to "optimize" pitching moment that added further drag reduction.

Regarding the efficiency of the CODISC process, the optimization portion typically required about twice as many design cycles as the initial CDISC-only design part. For the transonic wing design, which required the use of the more resource-intensive Navier-Stokes flow solver, beginning with the best-fit targets reduced the number of design cycles needed for the CDISC-only portion of the process to about half the time of the baseline analysis. Thus, the total design time was well within the goal of a factor of 5 over the time of a baseline analysis.

Finally, from an ease-of-use perspective, the ability to use the same primary flow constraint for either laminar or turbulent flow design for both transonic and supersonic speeds simplifies the knowledge base needed to set up new design cases. A new preprocessor has been developed that automatically sets up the CDISC input file with this constraint, along with a standard set of other flow and geometry constraints. The best-fit values are initially set as part of this process, then later automatically adjusted by CODISC to more optimal values. The robustness of this approach was demonstrated by starting one of the test case runs from a baseline with the wing twist and camber removed. Finally, some new CDISC constraints were proposed for improving the off-design performance for a single-point design, thus potentially reducing the need for a more complex multipoint design approach. Initial studies of these constraints used in airfoil designs showed promise, but further evaluations are needed with 3-D configurations.

Acknowledgments

This research is funded by the NASA Advanced Air Transport Technology Project in the Advanced Air Vehicles Program. Resources supporting some computational results in this paper were provided by the NASA High- End Computing (HEC) Program through the NASA Advanced Supercomputing (NAS) Division.

References

[1] Campbell, R.L., "Efficient Viscous Design of Realistic Aircraft Configurations," AIAA-98-2539, June 1998.
[2] Vassberg, John C.; Jameson, Antony; Peigin; Epstein, Boris; Roman, Dino L.; and Harrison, Neal A.: "A Pilot Project in Preparation of an Aerodynamic Optimization Workshop with Lessons Learned", AIAA 2008-6266, August 2008.
[3] Campbell, Richard L.; Viken, Sally A.; and Lynde, Michelle N.: "Application of Passive Drag Reduction Methods to a Generic Strut-Braced Wing". Presented at the PADRI Workshop, Barcelona, Spain, November 2017. https://www.scipedia.com/public/Pons_Prats_2017a
[4] Kenway, Gaetan; Housman, Jeffery; and Kiris, Cetin: "NASA Ames Research Center Contributions to the PADRI workshop". Presented at the PADRI Workshop, Barcelona, Spain, November 2017. https://www.scipedia.com/public/Kenway_et_al_2018a
[5] Campbell, Richard L.: "An Approach to Constrained Aerodynamic Design with Application to Airfoils", NASA TP-3260, November 1992.
[6] Wick, Andrew T.; Hooker, John R.; Hardin, Christopher J.; and Zeune, Cale H.: "Integrated Aerodynamic Benefits of Distributed Propulsion", AIAA 2015-1500, January 2015.
[7] Wick, Andrew T.; Hooker, John R.; Walker, Jimmy; Chan, David T.; Plumley, Ryan W.; and Zeune, Cale H.: "Hybrid Wing Body Performance Validation at the National Transonic Facility", AIAA 2017-0099, January 2017.
[8] Drela, Mark: Newton Solution of Coupled Viscous/Inviscid MultiElement Airfoil Flows, AIAA 90-1470, June 1990.
[9] Aftosmis, M. J., Berger, M. J., and Adomavicius, G.: "A Parallel Multilevel Method for Adaptively Refined Cartesian Grids With Embedded Boundaries", AIAA 2000–808, January 2000.
[10] Frink, N.T., Pirzadeh, S.Z., Parikh, P.C., Pandya, M.J., and Bhat, M.K., "The NASA Tetrahedral Unstructured Software System," The Aeronautical Journal, Vol. 104, No. 1040, October 2000, pp.491-499.
[11] Lynde, Michelle N. and Campbell, Richard L., "Expanding the Natural Laminar Flow Boundary for Supersonic Transports", AIAA 2016-4327, June 2016.
[12] Lynde, Michelle N., and Campbell, Richard L., "Computational Design and Analysis of a Transonic Natural Laminar Flow Wing for a Wind Tunnel Model", AIAA 2017-3058, June 2017.
[13] Campbell, Richard L.; and Lynde, Michelle N.: "Development of a Knowledge-Based Optimization Method for Aerodynamic Design", Presented at the RAeS Applied Aerodynamics Conference #787, July 2018, Bristol, UK.
[14] Lynde, Michelle N.; and Campbell, Richard L.: "Application of a Knowledge-Based Optimization Method for Aerodynamic Design", Presented at the RAeS Applied Aerodynamics Conference #787, July 2018, Bristol, UK.
[15] Chang, C.-L., "The Langley Stability and Transition Analysis Code (LASTRAC): LST, Linear and Nonlinear PSE for 2-D, Axisymmetric, and Infinite Swept Wing Boundary Layers," AIAA 2003-0974, 2003.
[16] Li, W.; Krist, S.; and Campbell, R.: "Transonic Airfoil Shape Optimization in Preliminary Design Environment", AIAA 2004-4629, August 2004.
[17] Vassberg, John C.; DeHaan, Mark A.; Rivers, S. Melissa; and Wahls, Richard A.: "Development of a Common Research Model for Applied CFD Validation Studies", AIAA 2008-6919, August 2008.

[18] Kenway, Gaetan K. W.; and Martins, Joaquim R. R. A.: "Multipoint Aerodynamic Shape Optimization Investigations of the Common Research Model Wing", AIAA 2015-0264, January 2015.
[19] Burdette, David A.; Kenway, Gaetan K. W.; and Martins, Joaquin R. R. A.: "Performance Evaluation of a Morphing Trailing Edge Using Multipoint Aerostructural Design Optimization", AIAA 2016-0159, January 2016.
[20] Kenway, Gaetan K. W.; and Martins, Joaquim R. R. A.: "Aerodynamic Shape Optimization of the CRM Coonfiguration Including Buffet-Onset Conditions", AIAA 2016-1294, January 2016.